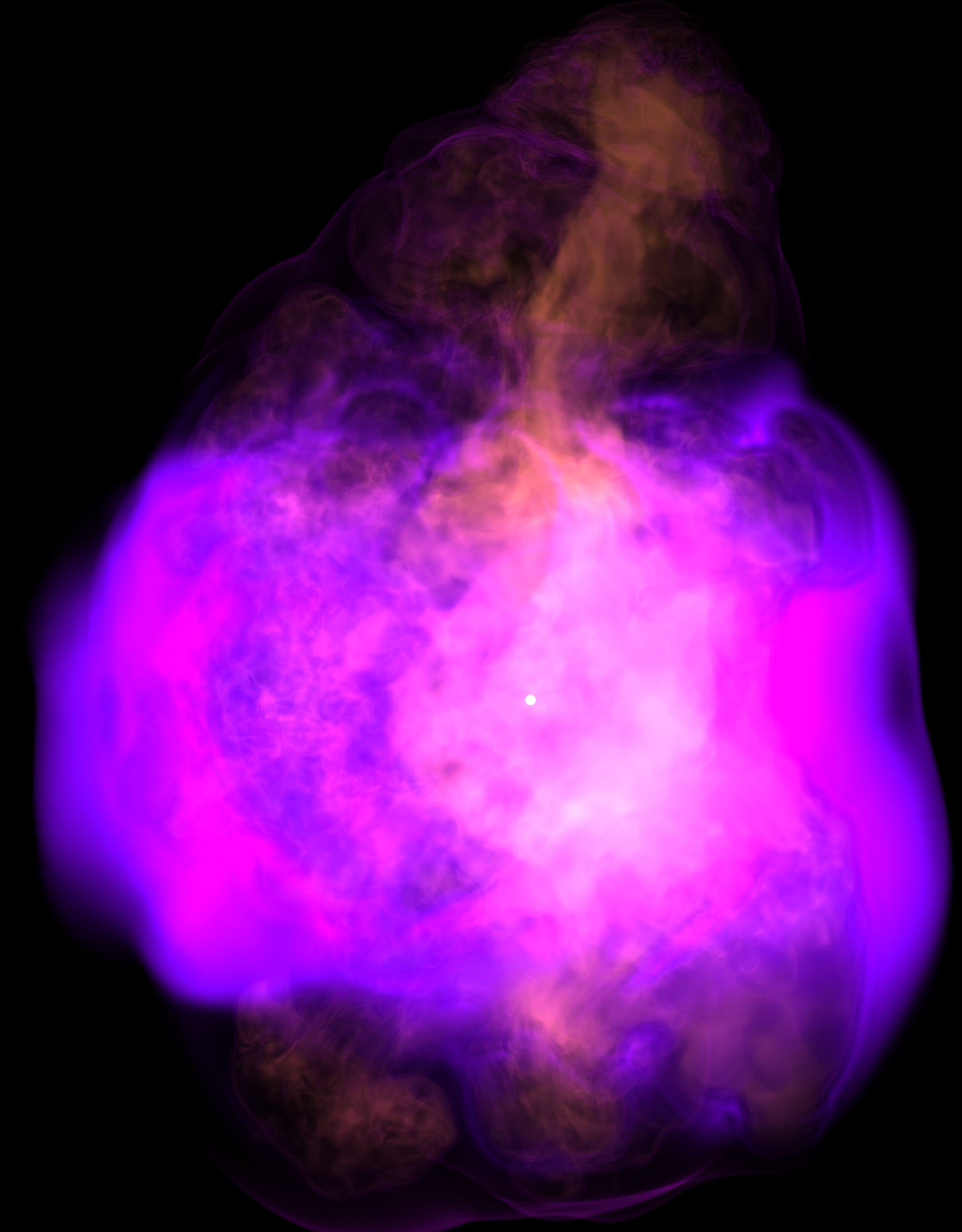
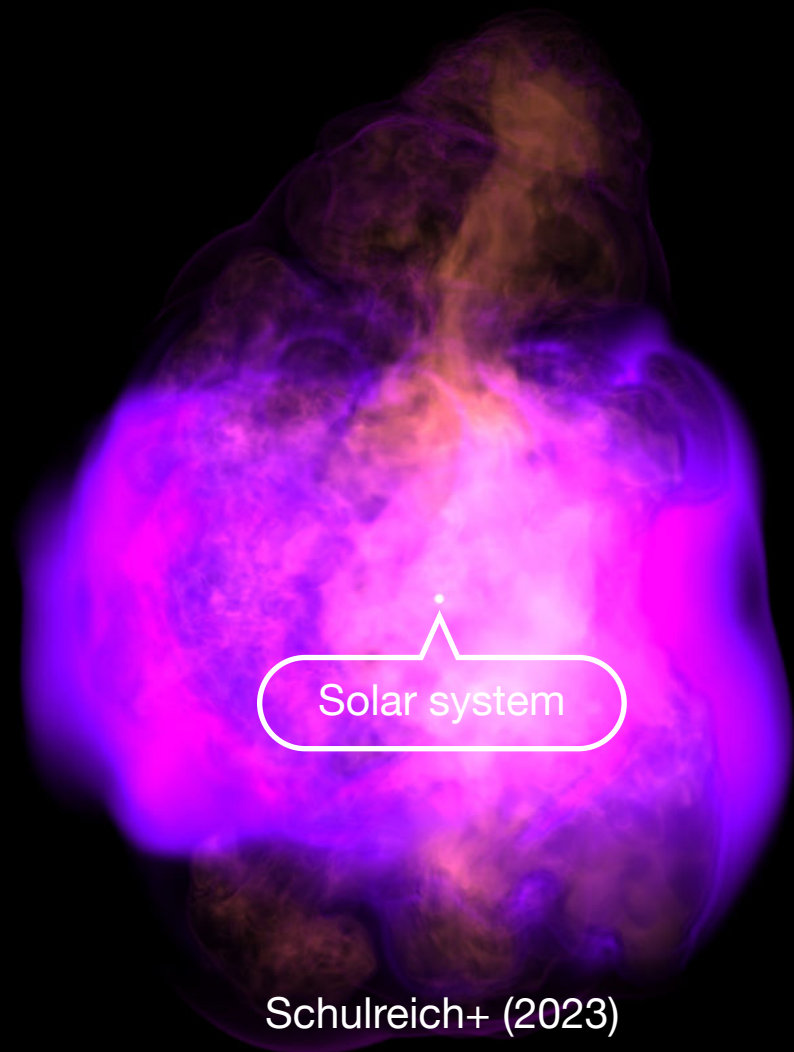


The supernova link between the Local Bubble and deep- sea radioisotopes

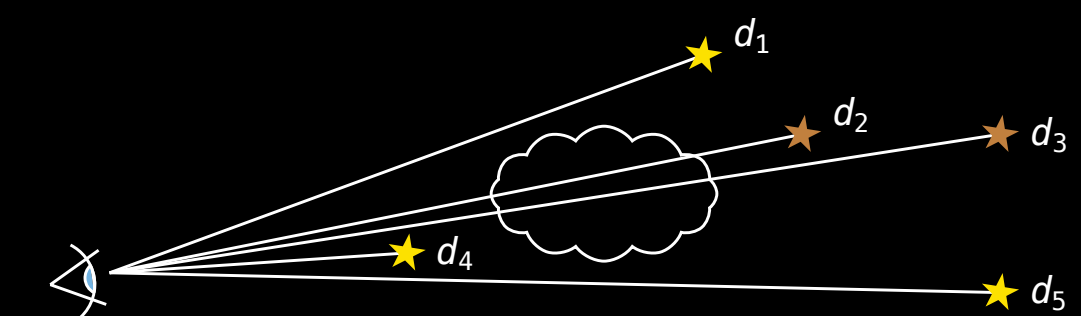
Michael M. Schulreich



The Local Bubble



Principle of dust extinction mapping



Schulreich+ (2023)

ROSAT all-sky survey 1/4 keV intensity

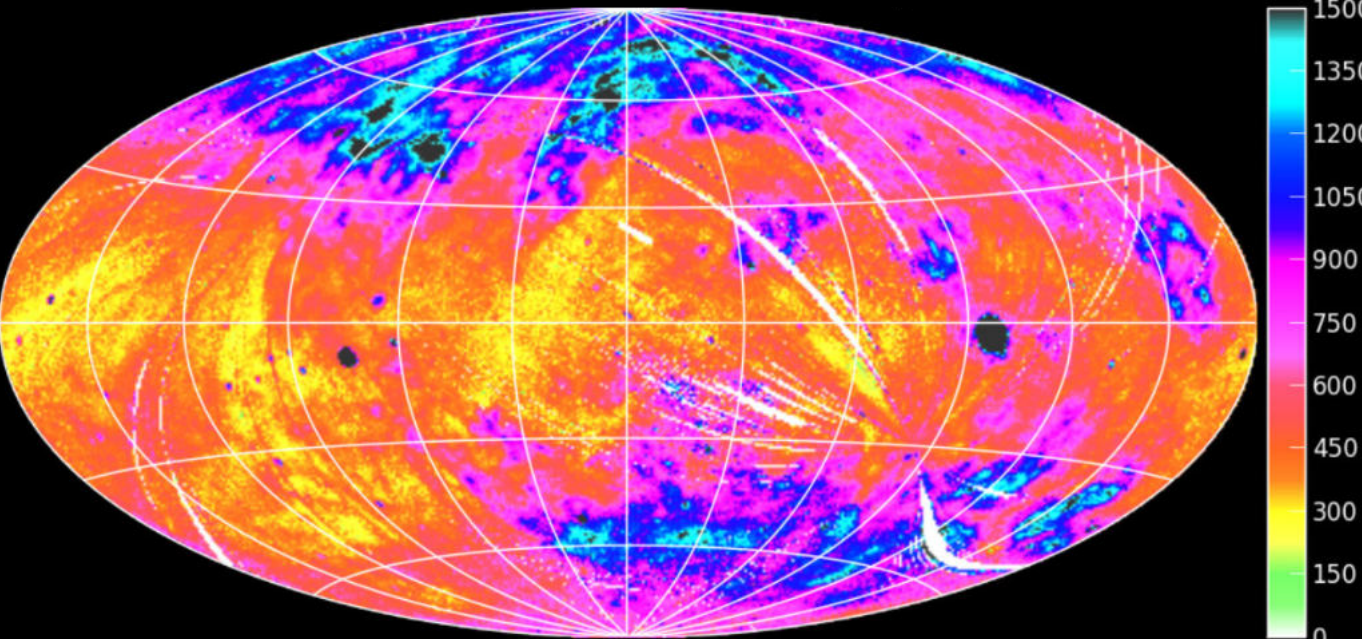
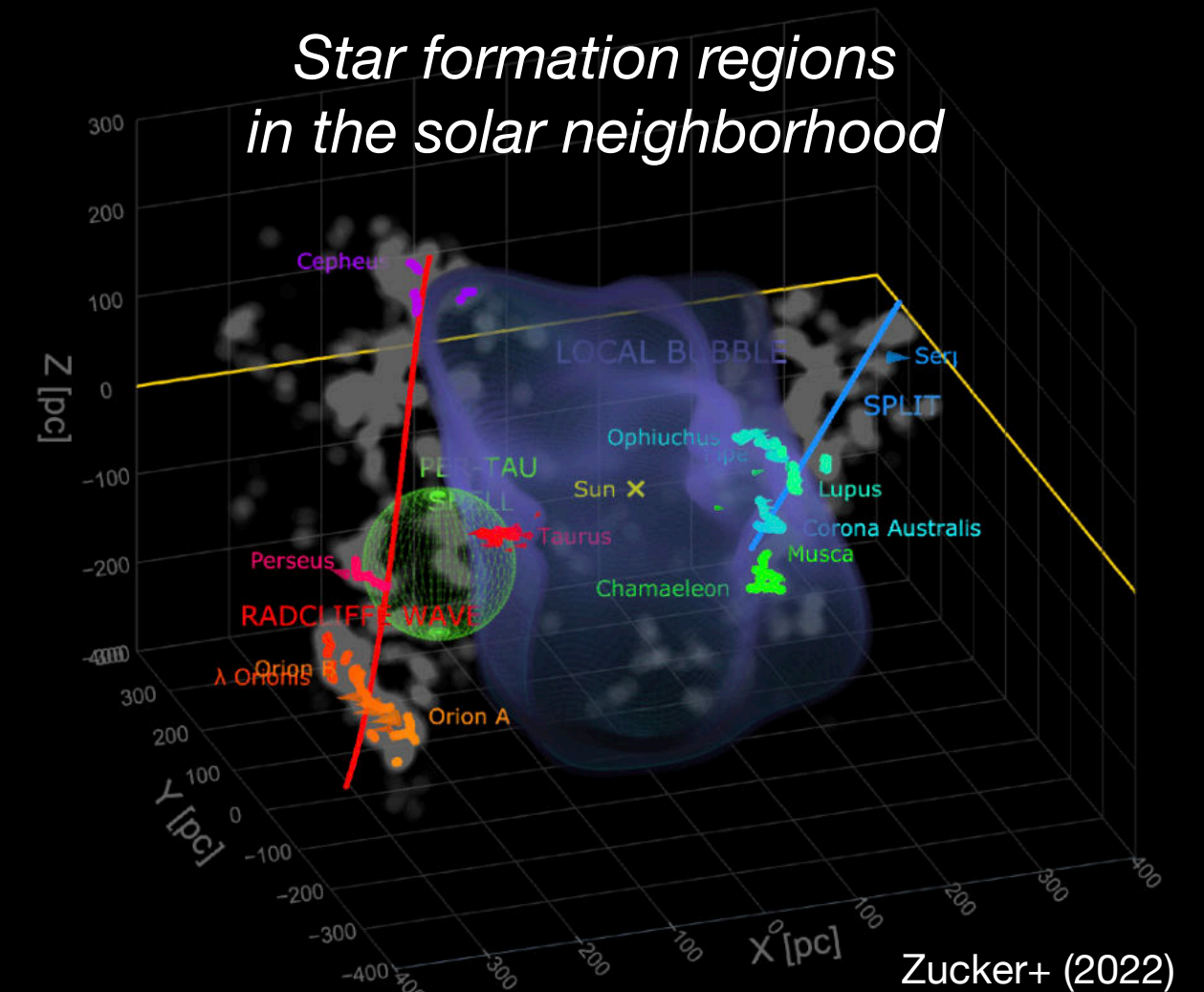


Image modified from Slavin+ (2016)



*Star formation regions
in the solar neighborhood*

Zucker+ (2022)

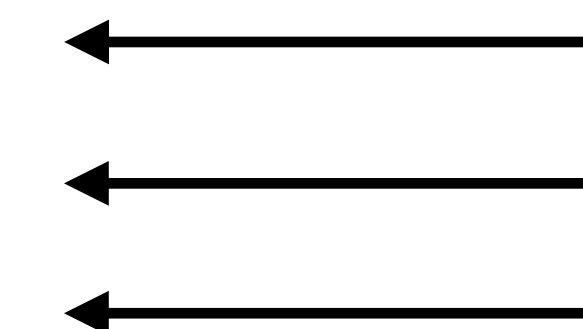
- **Cavity of low-density ($n < 0.005 \text{ cm}^{-3}$), high-temperature ($T \gtrsim 10^6 \text{ K}$) plasma surrounded by cold, dusty gas shell**
- Harbors the **solar system**
- Discovered, e.g., via Nal and Call absorption lines and dust extinction mapping
- **Extension:** $\sim 50\text{--}200 \text{ pc}$ into Galactic plane; $\gg 100 \text{ pc}$ perpendicular to it
- Hot LB plasma responsible for **majority of diffuse soft X-ray background**, first observed by sounding rockets and later by ROSAT and eROSITA
- Expanding LB shell probably **triggered almost all nearby star formation**
- **Widely accepted origin: stellar winds and supernovae** from nearby massive stars
- **But:** no OB association ***inside*** present LB!
 - ➡ Young star cluster must have passed through today's LB region **in the past**, providing enough SNe to inflate LB in the process

Unravelling the supernovae of the Local Bubble

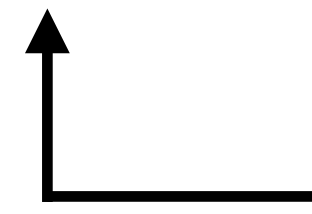
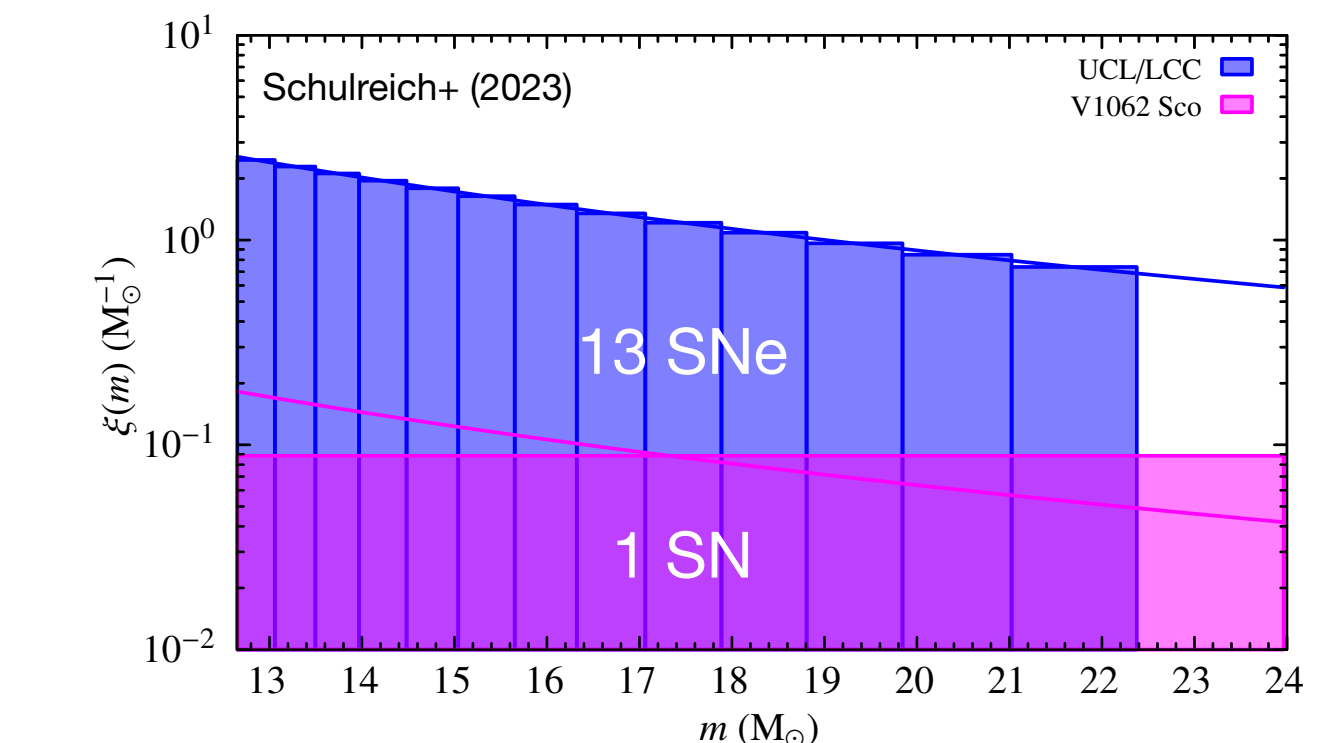
Recent near-Earth SNe:

- How many?
- When?
- Where?

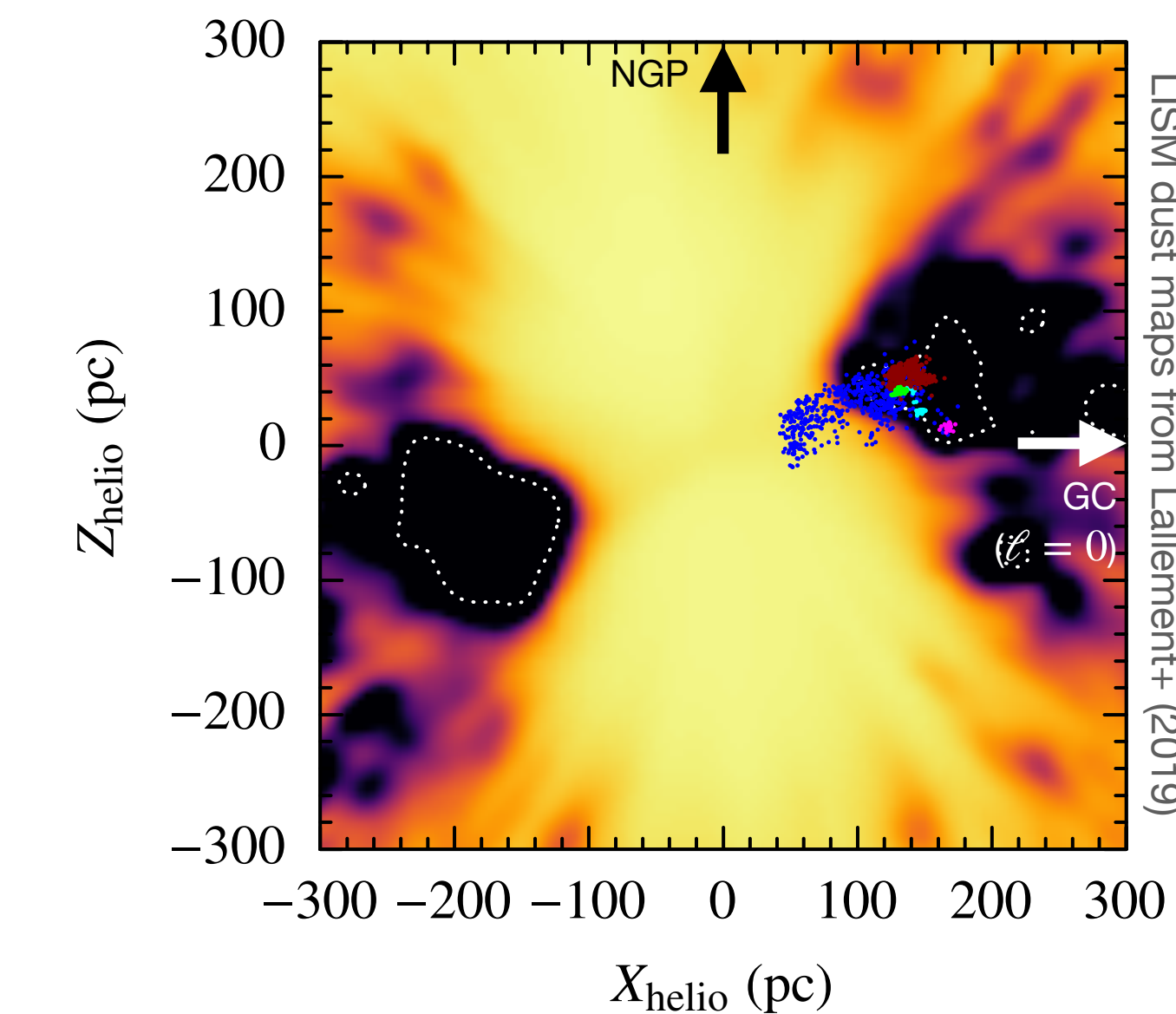
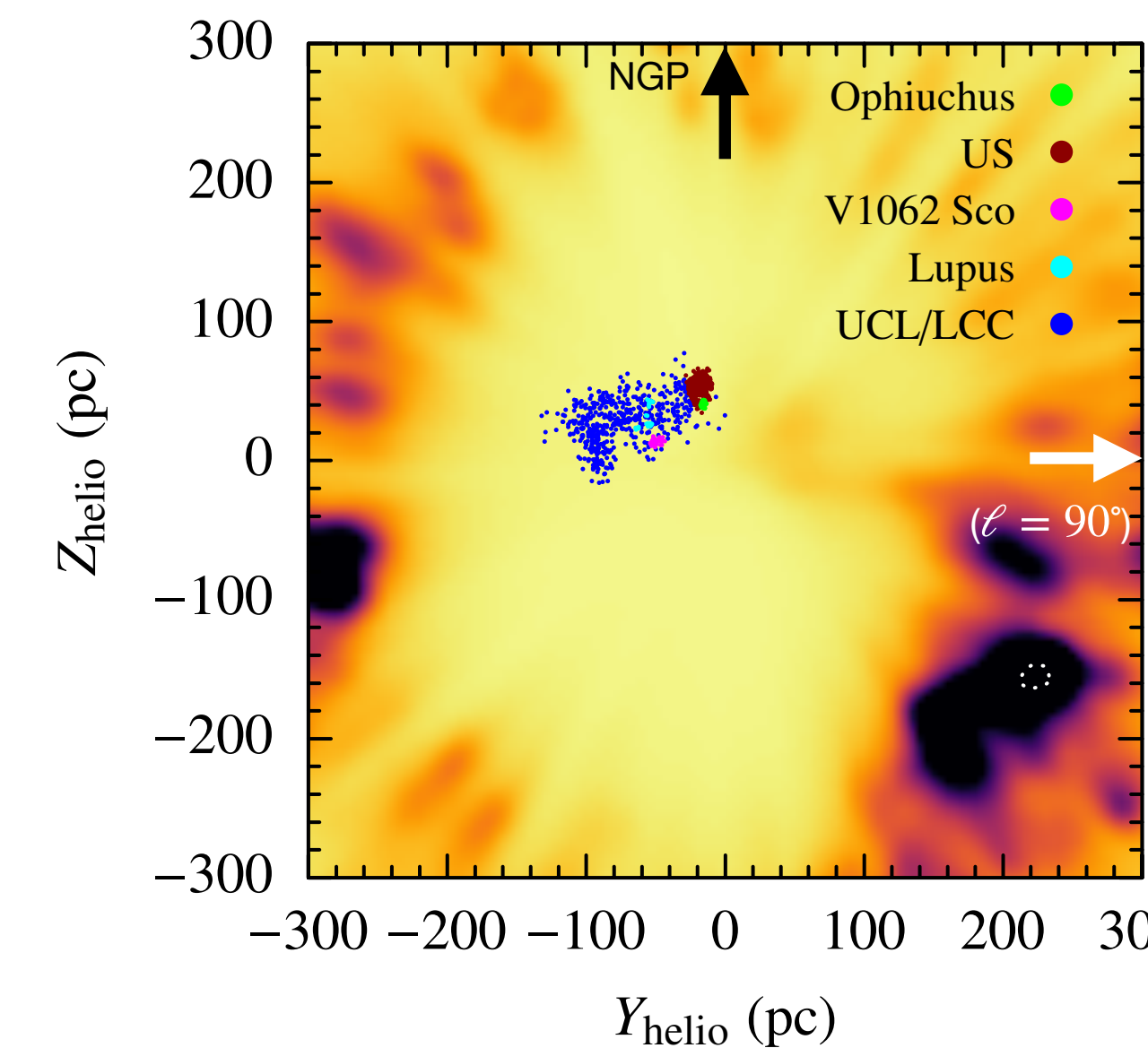
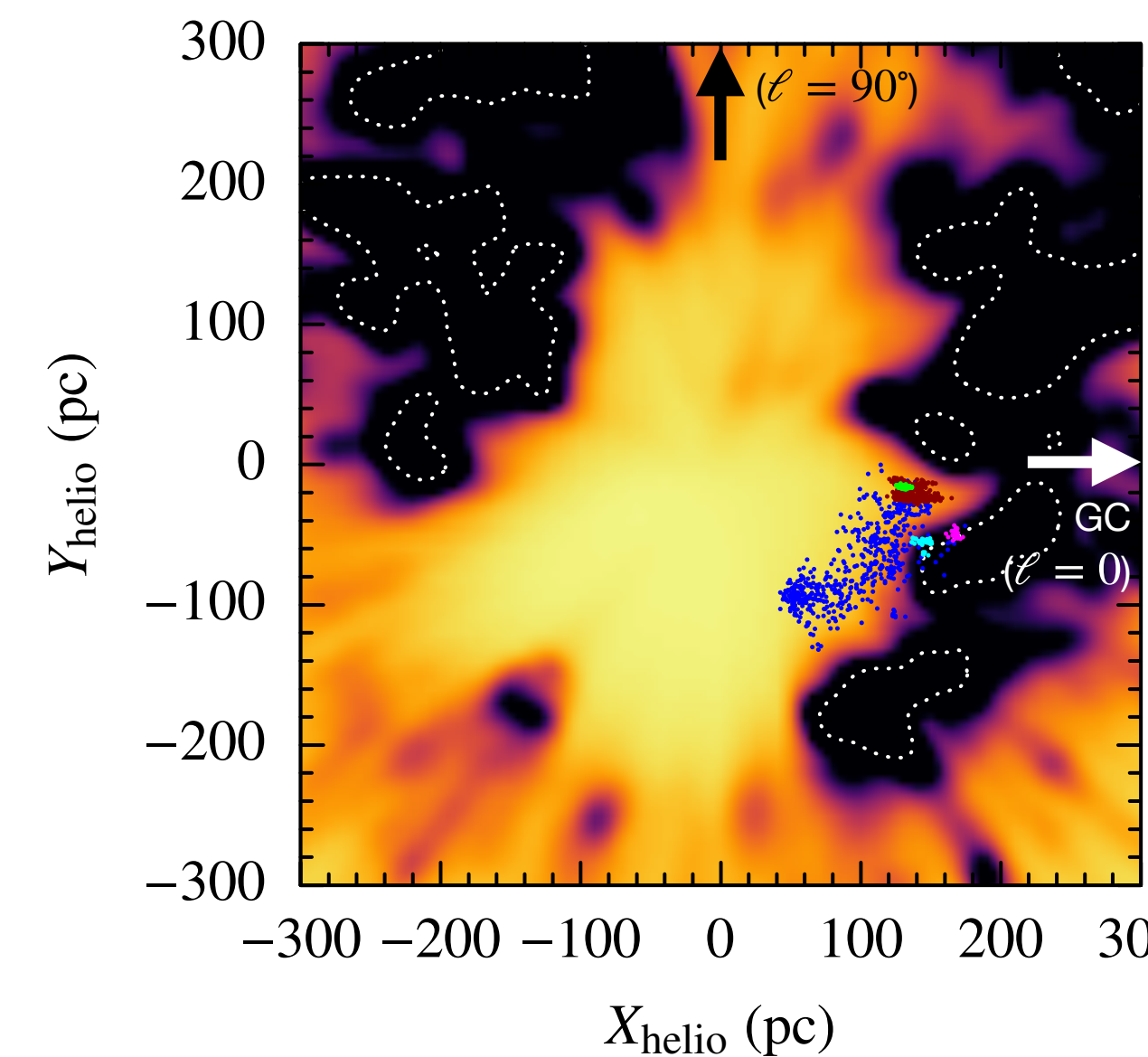
Suitable sample of stars provided



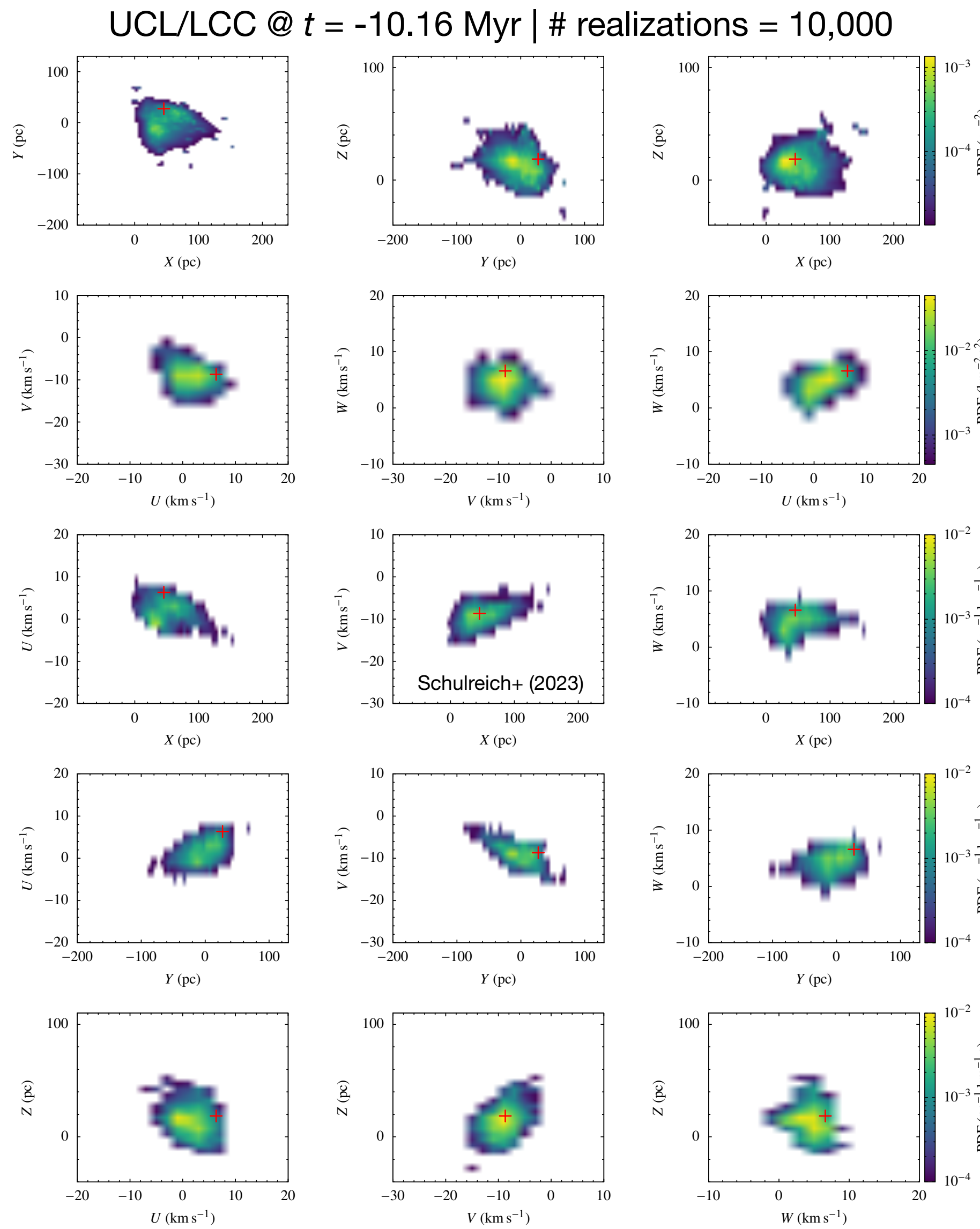
IMF fitting (Kroupa 2001)
rotating stellar evolution models (Ekström+ 2012)
stellar tracebacks in a Monte Carlo fashion



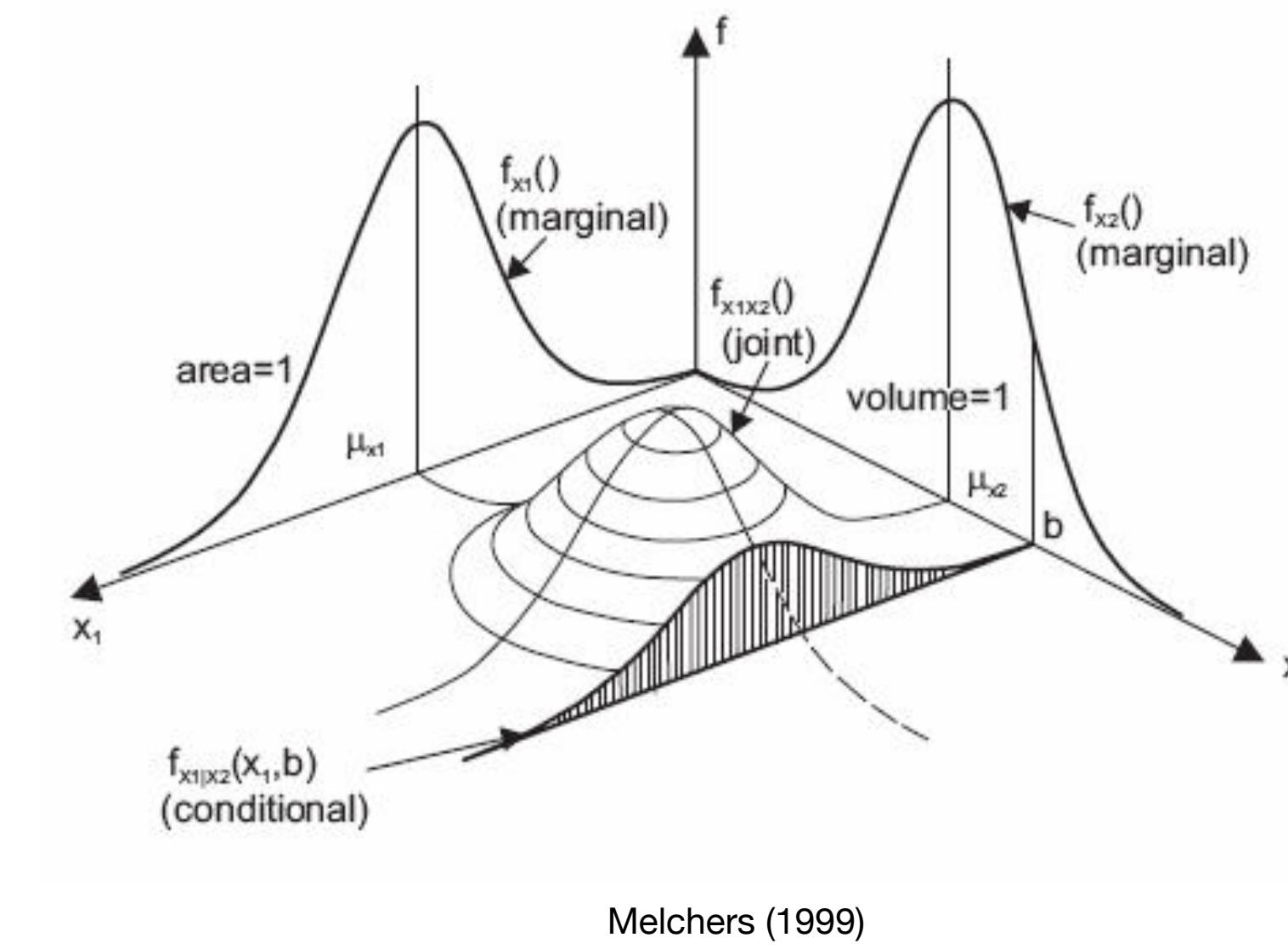
Sco-Cen complex populations extracted from *Gaia* EDR3 (Luhman 2022)



Marginal phase-space PDFs for Sco-Cen populations

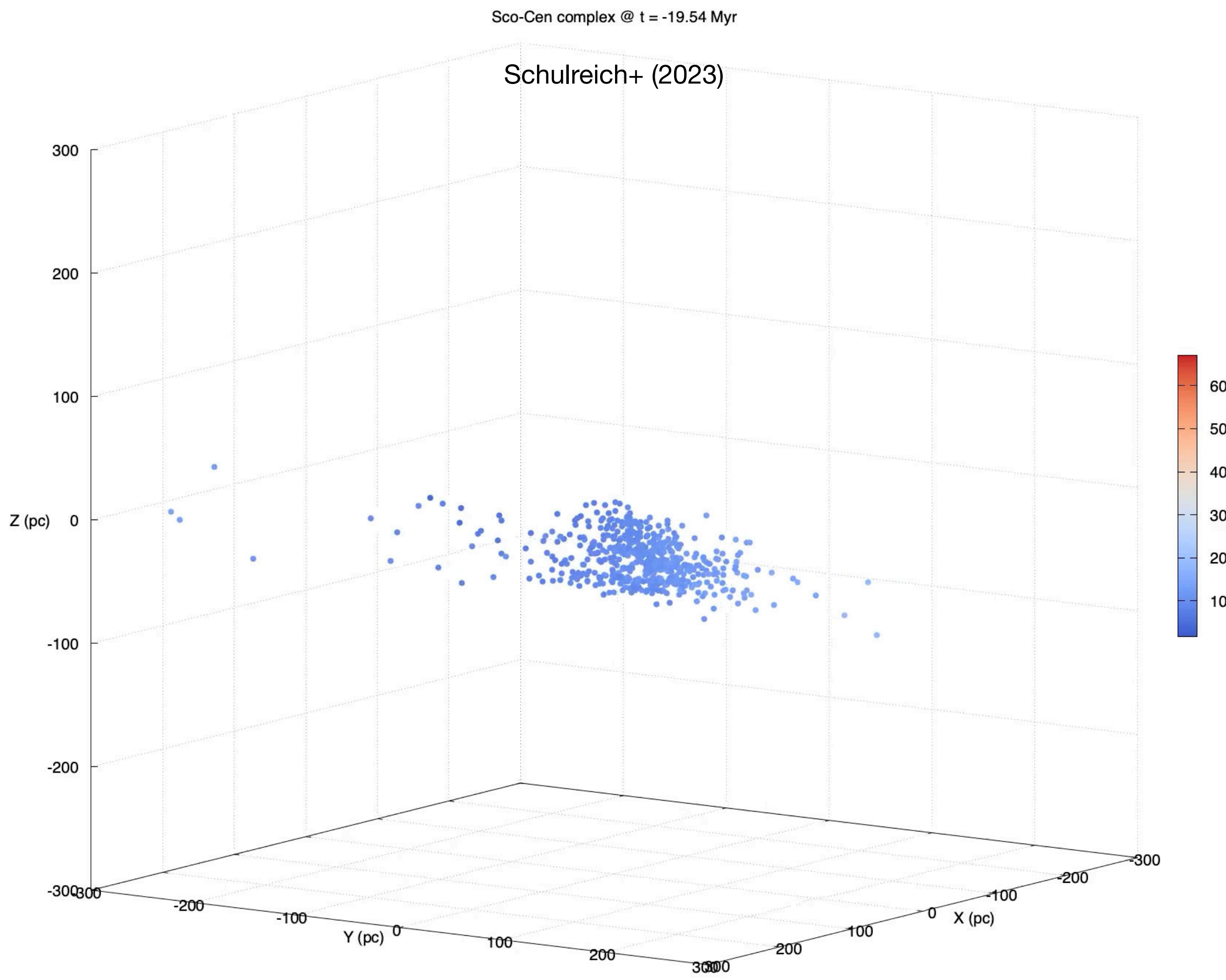


Joint and marginal probability density functions (PDFs)



Red crosses = phase-space coordinates of massive star just before its explosion (maximum of 6D PDF)
 ➡ sets entire trajectory of (wind-blowing) SN progenitor

Test particle simulations



- Gray sphere = LB approximated as a very large Weaver+ (1977) wind-blown bubble, neglecting its wind-driven phase

- Mechanical luminosity of SNe:

$$L_{\text{SN}} = \frac{E_{\text{SN}}}{\Delta t_{\text{exp}}} \approx (4.44 \times 10^{37} \text{ erg s}^{-1}) \left(\frac{E_{\text{SN}}}{10^{51} \text{ erg}} \right) \times \left(\frac{\Delta t_{\text{exp}}}{0.71 \text{ Myr}} \right)^{-1}$$

- LB radius evolution law:

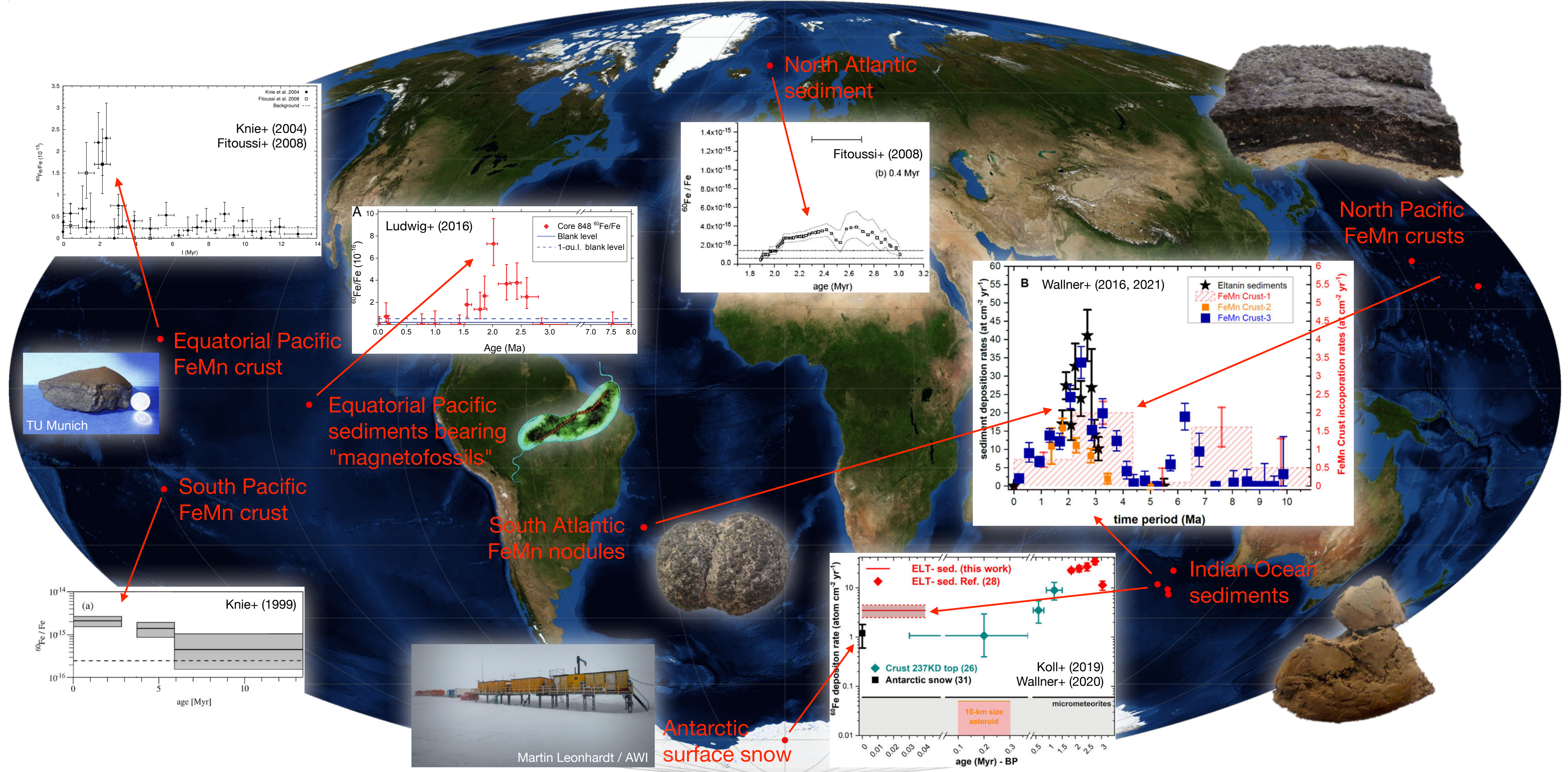
$$R = \left(\frac{125}{154 \pi} \right)^{1/5} \left(\frac{L_{\text{SN}}}{\rho_0} \right)^{1/5} t_{\text{SN}}^{3/5} \approx (241 \text{ pc}) \left(\frac{L_{\text{SN}}}{4.44 \times 10^{37} \text{ erg s}^{-1}} \right)^{1/5} \left(\frac{n_{\text{H},0}}{0.7 \text{ cm}^{-3}} \right)^{-1/5} \times \left(\frac{t_{\text{SN}}}{10.16 \text{ Myr}} \right)^{3/5}$$

Radioisotopic tracers

Isotope	Half-life (Myr)	Decay mode	Nucleosynthesis process	Background	Measurement efforts
^{60}Fe	$2.61 \pm 0.04^{1,2}$	β^-	s- and r-process (S)AGB stars, EC & CC SNe	✗	Detection in FeMn crusts ^{3,4,5,6,7} and nodules ⁶ , deep-ocean sediments ^{8,9} , Antarctic snow ¹⁰ , lunar regolith ¹¹ , diffuse Galactic γ -ray emission ¹² , and Galactic cosmic rays ¹³
					Negligible influx from sources other than SNe
					Courtesy of kurzgesagt.org

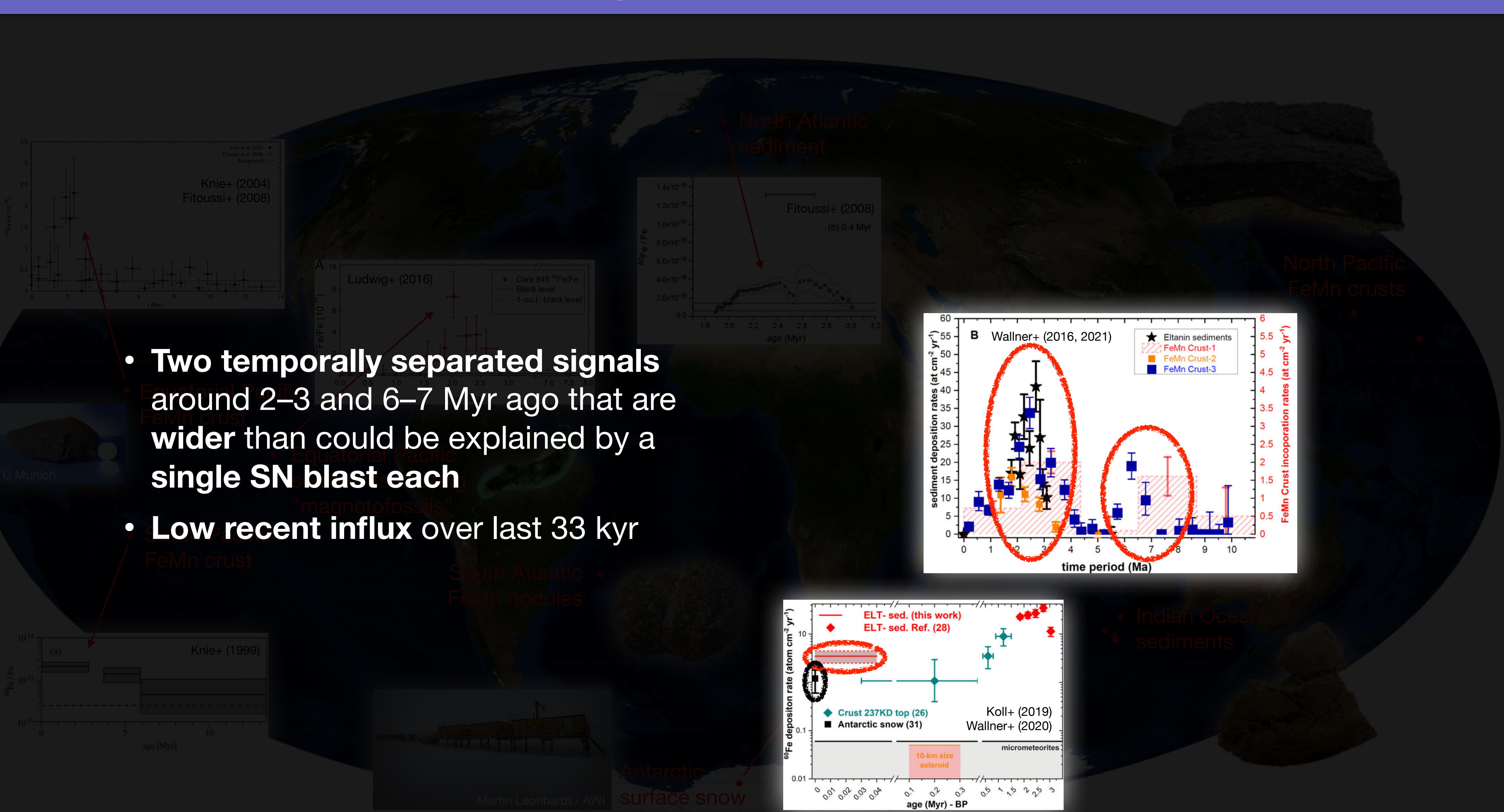
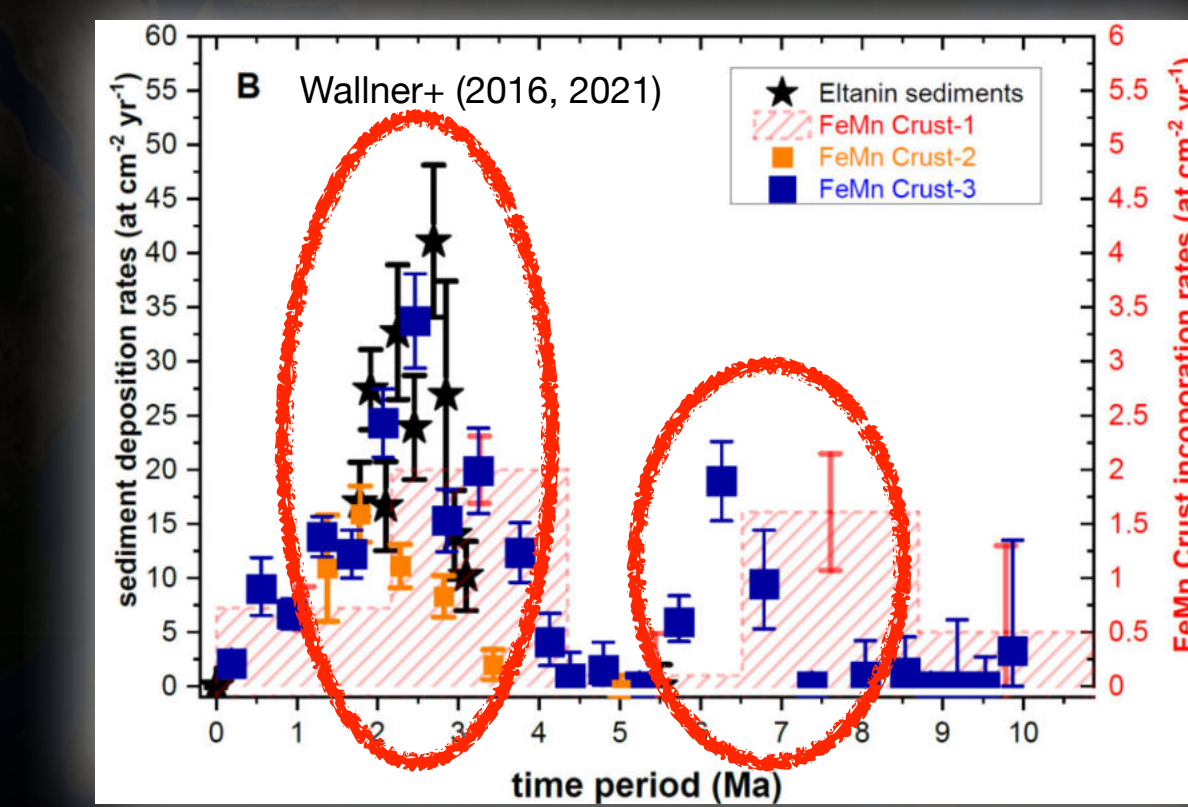
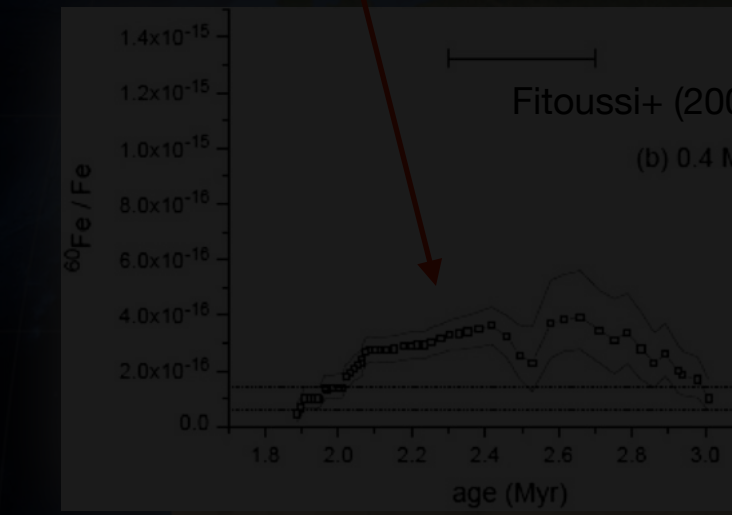
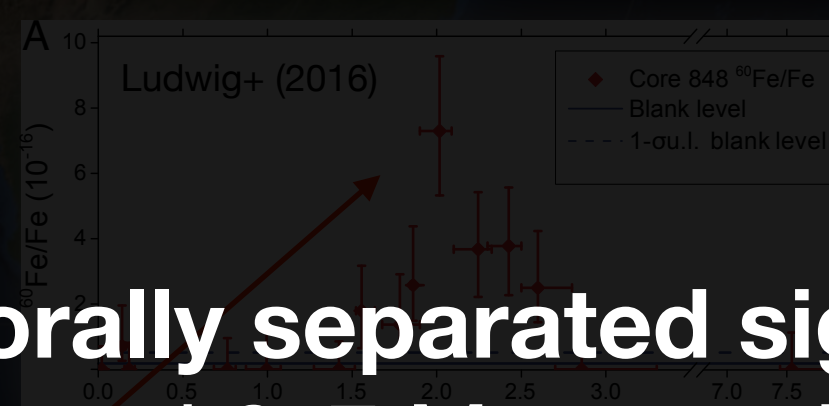
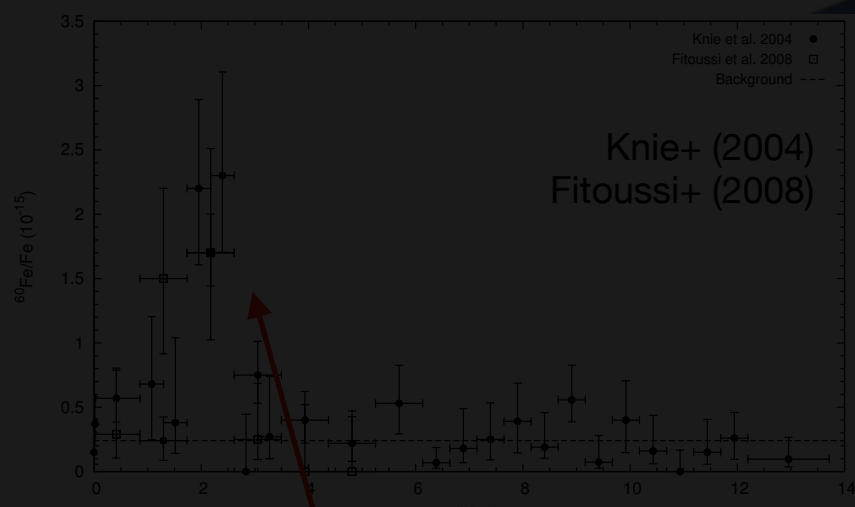
¹ Rugel+ (2009); ² Wallner+ (2015); ³ Knie+ (1999); ⁴ Knie+ (2004); ⁵ Fitoussi+ (2008); ⁶ Wallner+ (2016); ⁷ Wallner+ (2021); ⁸ Ludwig+ (2016); ⁹ Wallner+ (2020); ¹⁰ Koll+ (2019); ¹¹ Fimiani+ (2016); ¹² Wang+ (2007); ¹³ Binns+ (2016); ¹⁴ Basunia & Hurst (2016); ¹⁵ Feige+ (2018); ¹⁶ Plüsckie+ (2001); ¹⁷ Honda & Imamura (1971); ¹⁸ Korschinek+ (2020); ¹⁹ Nesaraja (2017)

^{60}Fe signatures on Earth ...

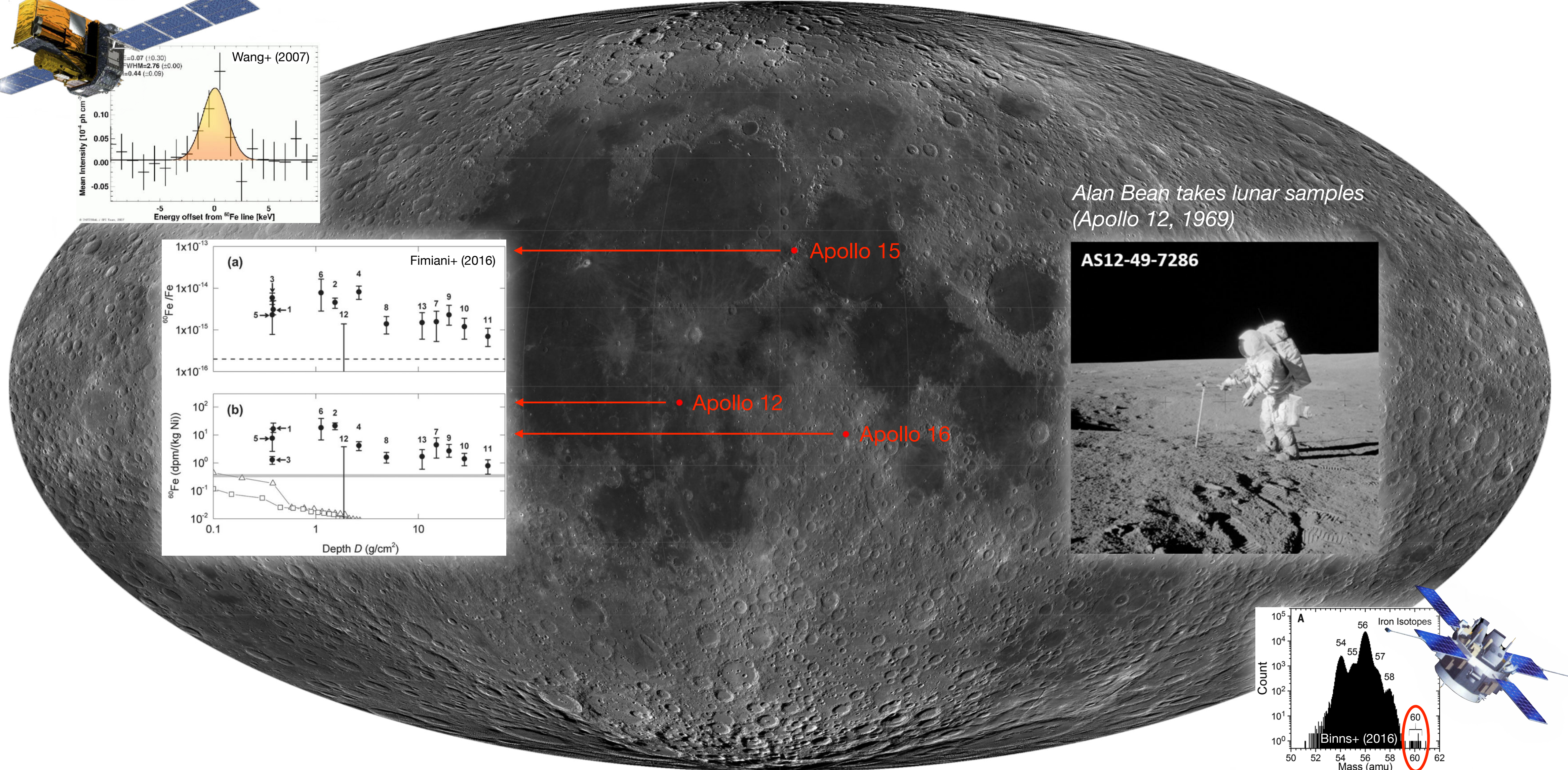
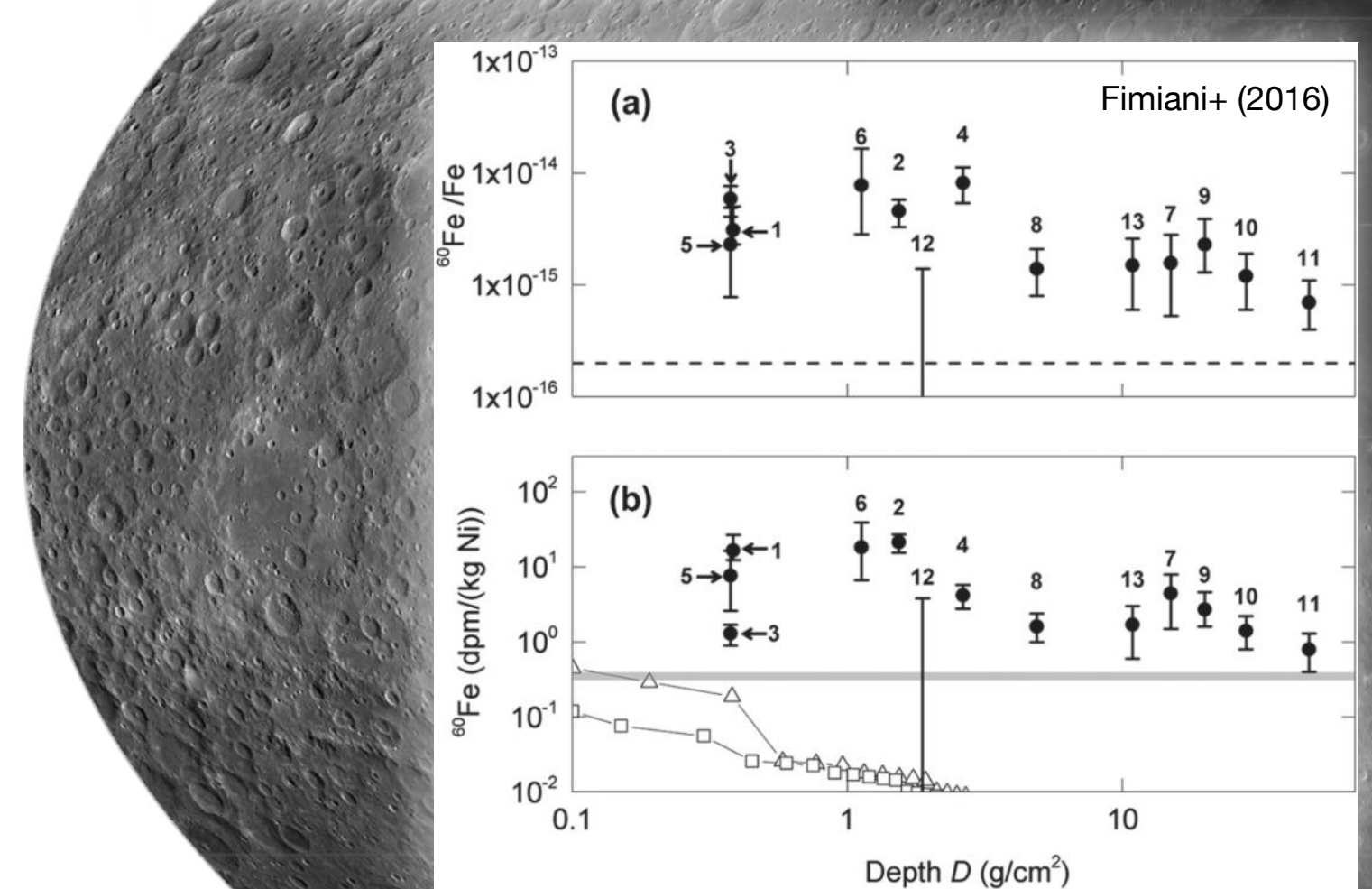
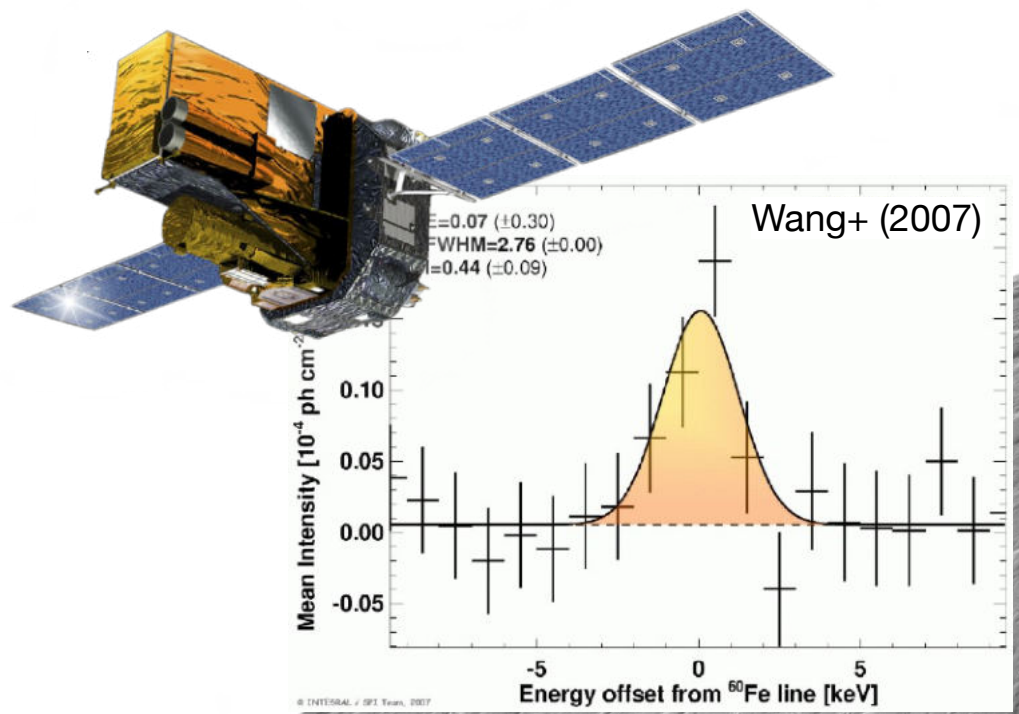


^{60}Fe signatures on Earth ...

- Two temporally separated signals around 2–3 and 6–7 Myr ago that are wider than could be explained by a single SN blast each
- Low recent influx over last 33 kyr



... and beyond

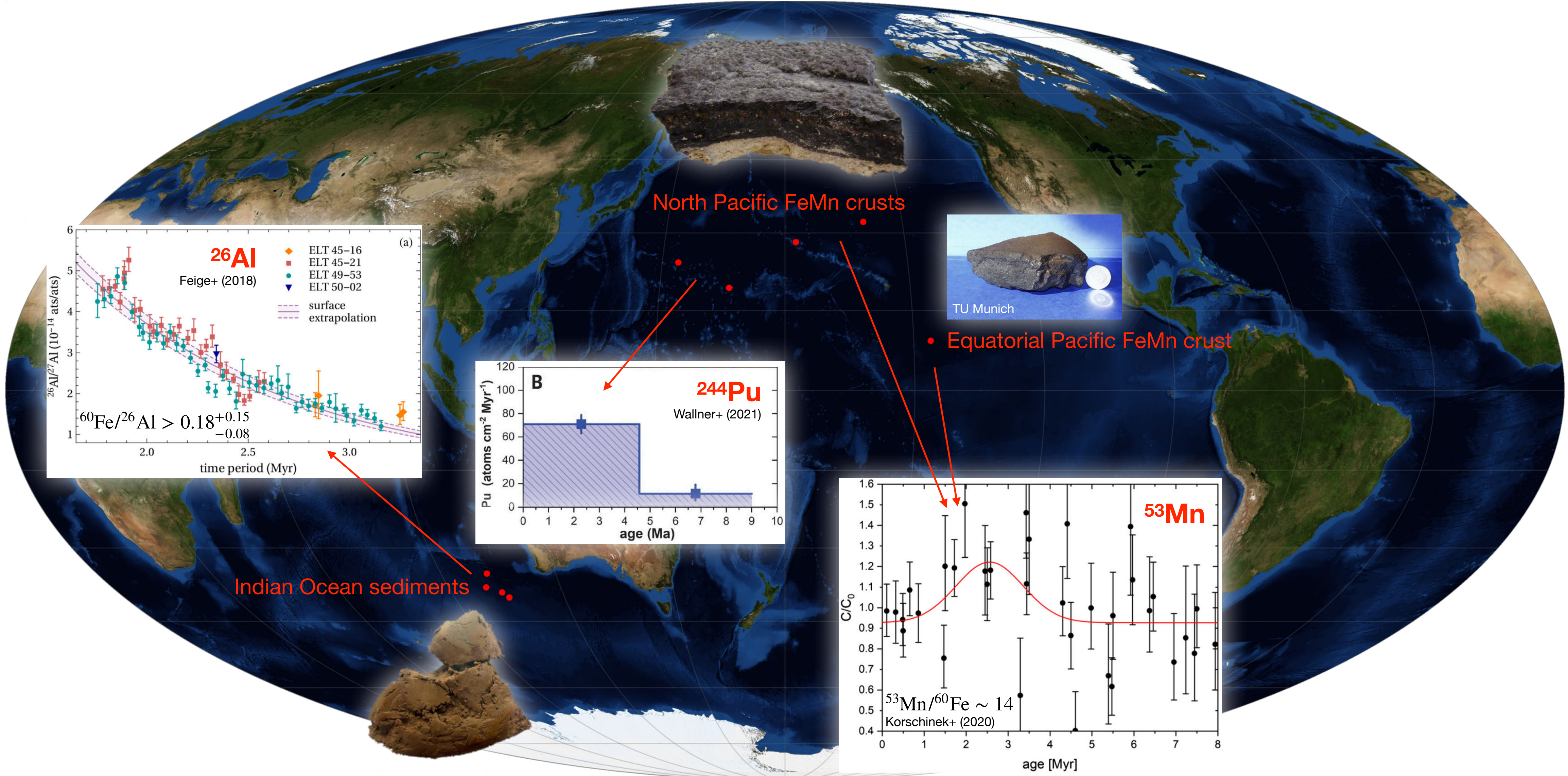


Radioisotopic tracers

Isotope	Half-life (Myr)	Decay mode	Nucleosynthesis process	Background	Measurement efforts
^{60}Fe	$2.61 \pm 0.04^{1,2}$	β^-	s- and r-process (S)AGB stars, EC & CC SNe	✗	Detection in FeMn crusts ^{3,4,5,6,7} and nodules ⁶ , deep-ocean sediments ^{8,9} , Antarctic snow ¹⁰ , lunar regolith ¹¹ , diffuse Galactic γ -ray emission ¹² , and Galactic cosmic rays ¹³ Negligible influx from sources other than SNe
^{26}Al	0.717 ± 0.024^{14}	β^+ , electron capture	$^{25}\text{Mg}(\text{p},\gamma)$ reaction (S)AGB & WR stars, CC SNe	✓	Searches in FeMn crusts ¹⁵ Detection in diffuse Galactic γ -ray emission ¹⁶
^{53}Mn	3.7 ± 0.4^{17}	Electron capture	Explosive Si & O burning CC SNe	✓	Evidence in FeMn crusts ¹⁸ Continuous influx from production in the Earth's atmosphere Continuous influx from production in IDPs

¹ Rugel+ (2009); ² Wallner+ (2015); ³ Knie+ (1999); ⁴ Knie+ (2004); ⁵ Fitoussi+ (2008); ⁶ Wallner+ (2016); ⁷ Wallner+ (2021); ⁸ Ludwig+ (2016); ⁹ Wallner+ (2020); ¹⁰ Koll+ (2019); ¹¹ Fimiani+ (2016); ¹² Wang+ (2007); ¹³ Binns+ (2016); ¹⁴ Basunia & Hurst (2016); ¹⁵ Feige+ (2018); ¹⁶ Pluschke+ (2001); ¹⁷ Honda & Imamura (1971); ¹⁸ Korschinek+ (2020); ¹⁹ Nesaraja (2017)

Signatures of other radioisotopes on Earth



Radioisotopic tracers

Isotope	Half-life (Myr)	Decay mode	Nucleosynthesis process	Background	Measurement efforts
^{60}Fe	$2.61 \pm 0.04^{1,2}$	β^-	s- and r-process (S)AGB stars, EC & CC SNe	✗ Negligible influx from sources other than SNe	Detection in FeMn crusts ^{3,4,5,6,7} and nodules ⁶ , deep-ocean sediments ^{8,9} , Antarctic snow ¹⁰ , lunar regolith ¹¹ , diffuse Galactic γ -ray emission ¹² , and Galactic cosmic rays ¹³
^{26}Al	0.717 ± 0.024^{14}	β^+ , electron capture	$^{25}\text{Mg}(\text{p},\gamma)$ reaction (S)AGB & WR stars, CC SNe	✓ Continuous influx from production in the Earth's atmosphere	Searches in FeMn crusts ¹⁵ Detection in diffuse Galactic γ -ray emission ¹⁶
^{53}Mn	3.7 ± 0.4^{17}	Electron capture	Explosive Si & O burning CC SNe	✓ Continuous influx from production in IDPs	Evidence in FeMn crusts ¹⁸
^{244}Pu	81.3 ± 0.3^{19}	α -decay: 99.88% Spontaneous fission: 0.12%	r-process CC SNe? KNe? MR SNe?	✓ Recent influx from anthropogenic production	Detection in FeMn crusts ⁷

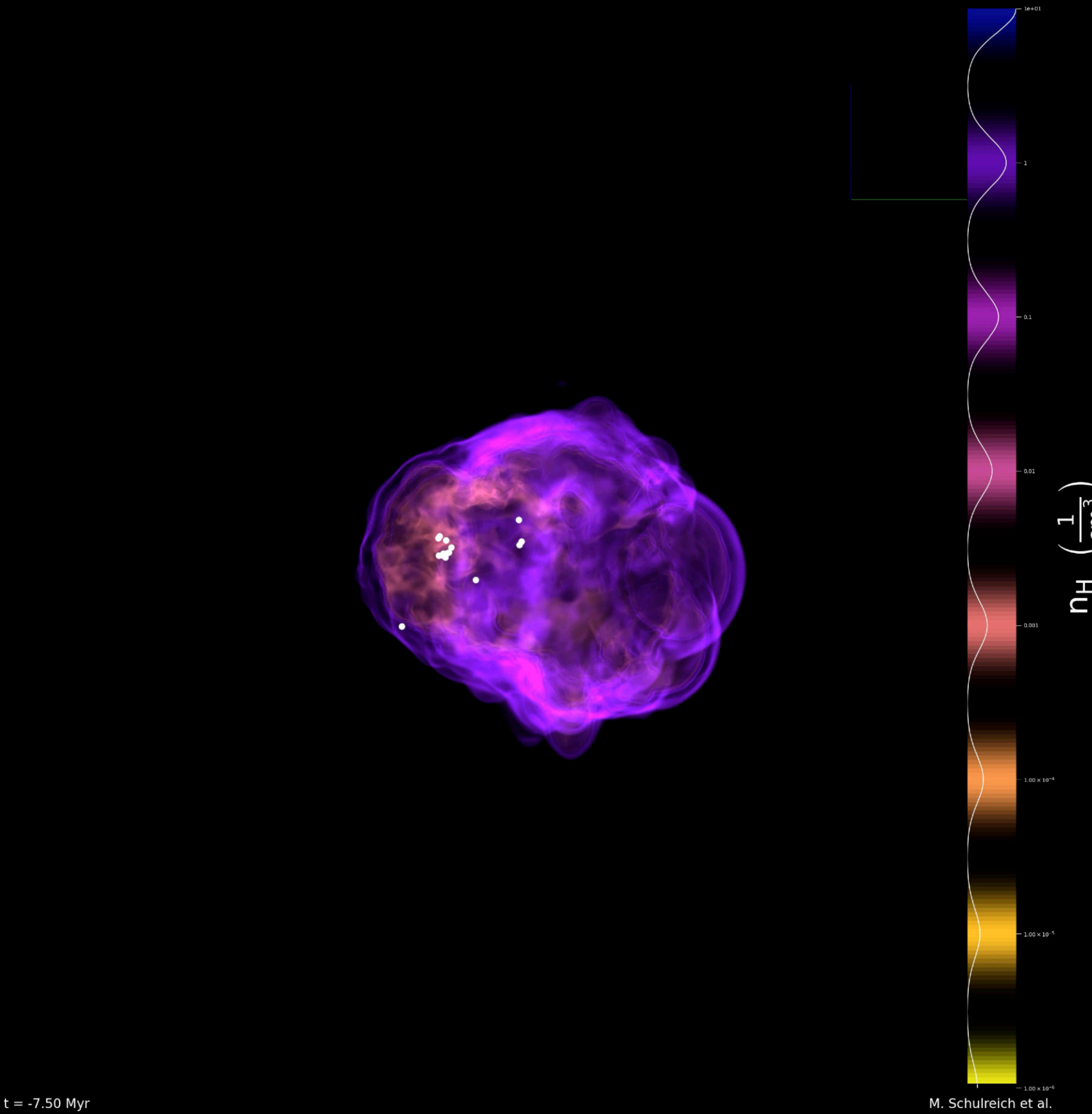
Measurements of these radioisotopes pose **additional constraints on the LB formation scenario**, which we further investigated by means of **3D hydrodynamic simulations**

¹Rugel+ (2009); ²Wallner+ (2015); ³Knie+ (1999); ⁴Knie+ (2004); ⁵Fitoussi+ (2008); ⁶Wallner+ (2016); ⁷Wallner+ (2021); ⁸Ludwig+ (2016); ⁹Wallner+ (2020); ¹⁰Koll+ (2019); ¹¹Fimiani+ (2016); ¹²Wang+ (2007); ¹³Binns+ (2016); ¹⁴Basunia & Hurst (2016); ¹⁵Feige+ (2018); ¹⁶Pluschke+ (2001); ¹⁷Honda & Imamura (1971); ¹⁸Korschinek+ (2020); ¹⁹Nesaraja (2017)

Hydrodynamic simulations

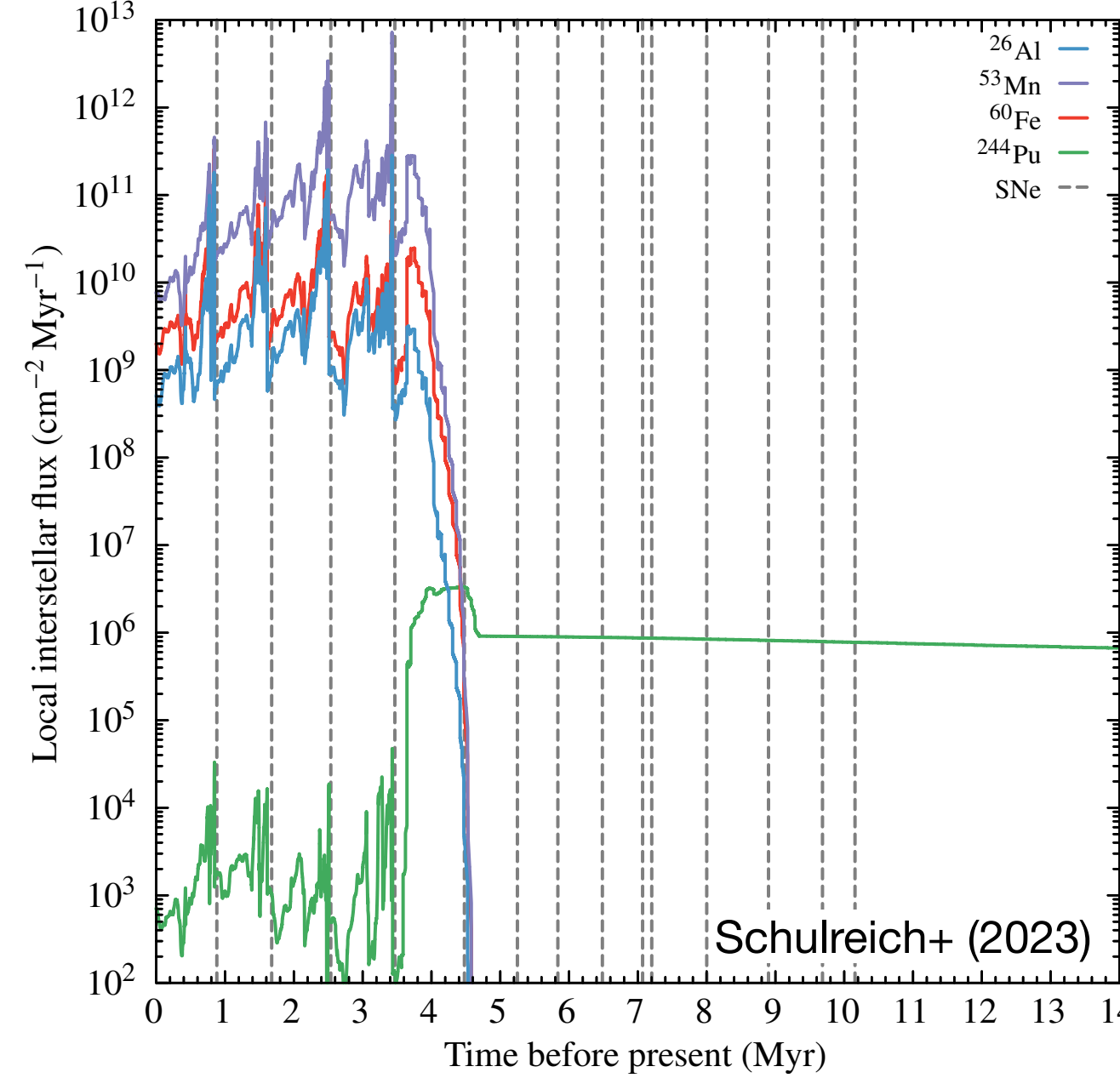
- performed with second-order Godunov-type tree-based AMR code RAMSES (Teyssier 2002)
- solve full 3D HD equations on cubic cutout of Galactic disk (800^3 pc 3) that co-rotates with LSR
- sub-parsec theoretical resolutions: ≤ 0.78 pc
- stratified background medium in hydrostatic and thermal equilibrium
- external gravitational field from Barros+ (2016)
- CIE cooling for gas with solar metallicity using GRACKLE cooling library (Smith+ 2017)
- collisionless particles:
 - massive stars: move along pre-calculated trajectories, blow (MS-/RSG-[/WR-]) winds, and explode as SNe when their lifetime has run out
 - Sun/Earth: represents "moving detector" for radioisotopic fluxes
- radioisotopes (^{26}Al , ^{53}Mn , ^{60}Fe , ^{244}Pu) treated as decaying passive scalars:
 - stellar-wind yields from Ekström+ (2012)
 - SN yields from Limongi & Chieffi (2018)

Hydrodynamic simulations

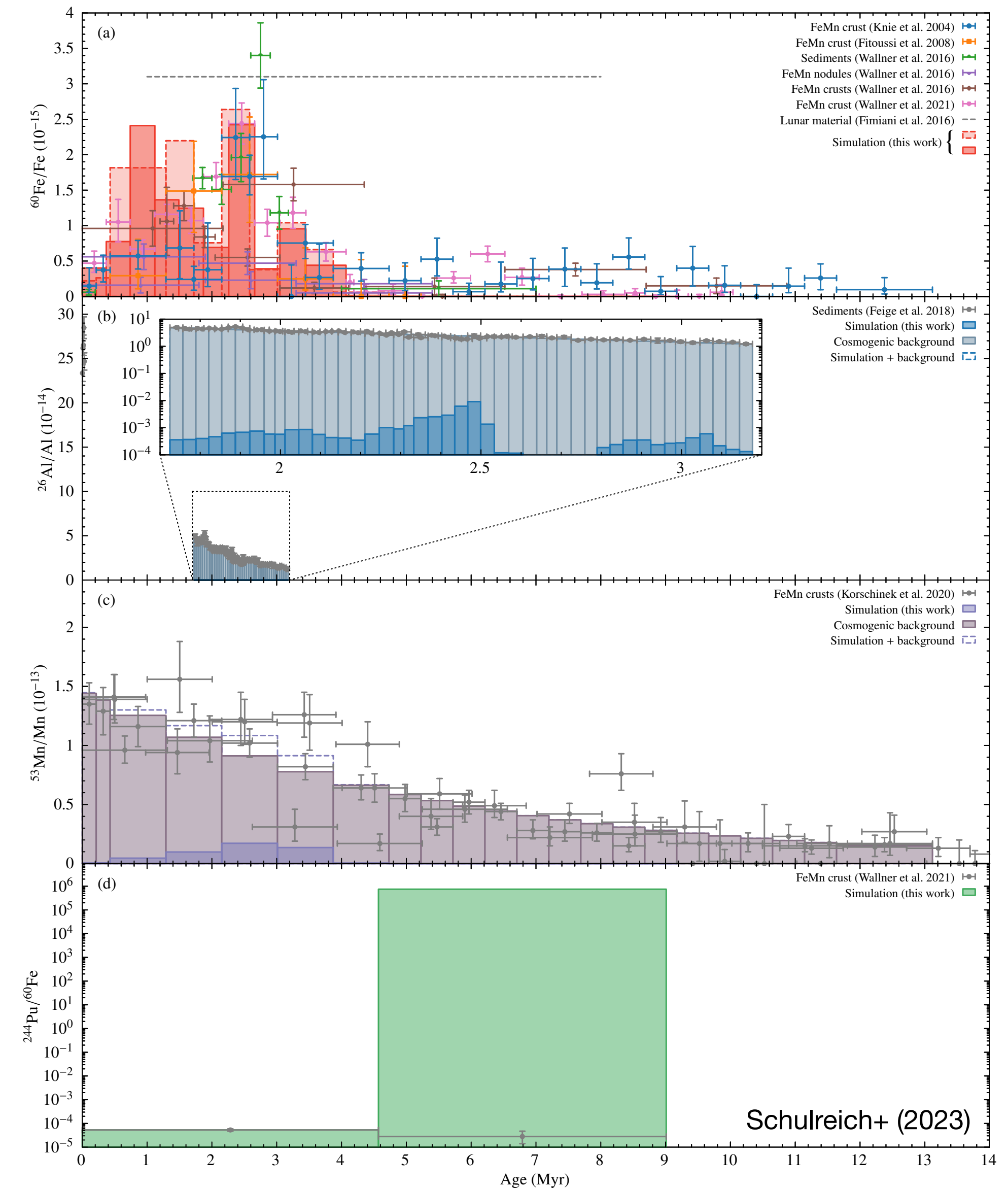


Comparison with radioisotopic measurements

$$F_i = \frac{\rho \tilde{u} C_i}{A_i m_u}$$

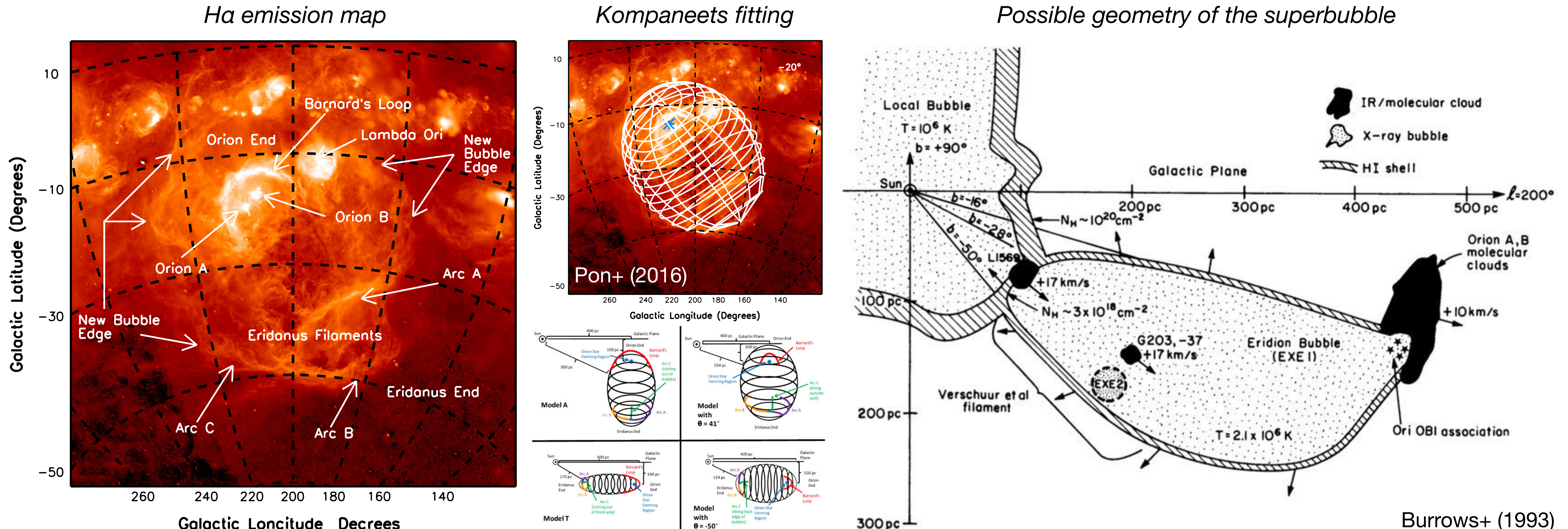


$$\frac{n_i(\Delta a_\ell)}{n_j} = \frac{1}{n_j} \frac{\frac{f_i}{4} \int_{a_{\ell,1}}^{a_{\ell,u}} F_i(a) \exp(-\lambda_i a) da}{\Delta d_\ell}$$

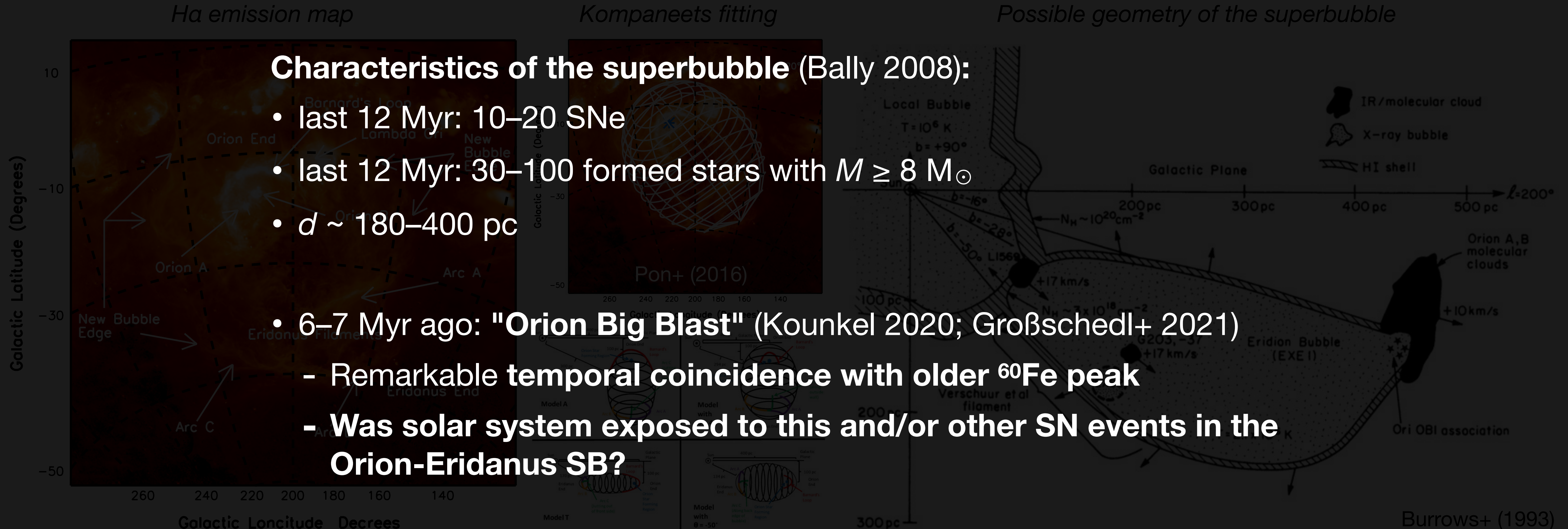


- **Current model nicely fits measurements before older peak** (younger peak generated by **SN blast waves & reflected shocks**), incl. **recent influxes** (generated by yet undecayed turbulence in LB cavity)
- **Older peak requires inclusion of neighboring superbubble** to be crossed by the solar system before entering the LB about 4.6 Myr ago

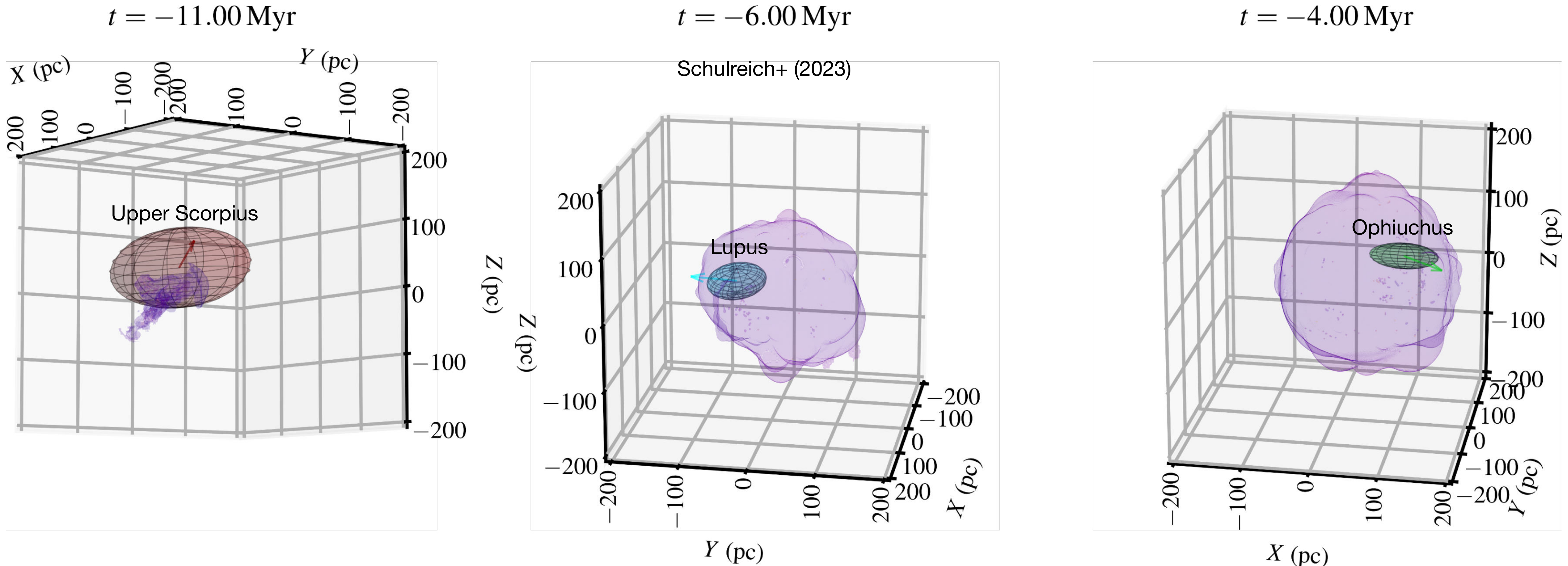
The Orion-Eridanus superbubble



The Orion-Eridanus superbubble



Presumed birthplaces of Sco-Cen subgroups w.r.t. evolving Local Bubble



LB could indeed have triggered star formation near the Sun through its expansion!

Takeaways

- Measurements of ^{26}Al , ^{53}Mn , ^{60}Fe , and ^{244}Pu in terrestrial archives – particularly a 2–4 Myr old ^{60}Fe peak – are consistent with the formation of the LB through a series of near-Earth SNe over the last ~10 Myr
- Stellar winds impact radioisotope distribution and LB dynamics
- The solar system entered the LB about 4.6 Myr ago
- Recent influx of ^{60}Fe in Antarctic snow and deep-sea sediments explained by turbulent radioisotopic transport, primarily from SN explosions and LB shell reflections
- Support for the hypothesis that the LB triggered star formation in the solar vicinity through its expansion
- Second, separate ^{60}Fe peak measured at 6–9 Myr ago presumably resulted from the solar system passing through a neighboring cavity (the Orion-Eridanus superbubble?), before settling in the LB

A&A, 680, A39 (2023)
<https://doi.org/10.1051/0004-6361/202347532>
© The Authors 2023

**Astronomy
&
Astrophysics**

Numerical studies on the link between radioisotopic signatures on Earth and the formation of the Local Bubble

II. Advanced modelling of interstellar ^{26}Al , ^{53}Mn , ^{60}Fe , and ^{244}Pu influxes as traces of past supernova activity in the solar neighbourhood

M. M. Schulreich¹ , J. Feige^{1,2}, and D. Breitschwerdt¹

